Available online at www.sciencedirect.com
ScienceDirect
Journal of Molecular Catalysis A: Chemical 276 (2007) 197–204
JOURNAL OF MOLECULAR CATALYSIS A: CHEMICAL
www.elsevier.com/locate/molcata

Influence of alkaline earth metal on acid–base characteristics of V_2O_5/MO–TiO_2 (M = Ca, Sr and Ba) catalysts

Benjaram M. Reddy *, Katuri J. Ratnam, Pranjal Saikia, Gode Thrimurthulu

Inorganic and Physical Chemistry Division, Indian Institute of Chemical Technology, Hyderabad 500007, India

Received 9 May 2007; received in revised form 25 June 2007; accepted 6 July 2007
Available online 17 July 2007

Abstract

The influence of various alkaline earth metal oxides (CaO, SrO and BaO) on the acid–base properties of TiO_2 and the dispersion behaviour of V_2O_5 over MO−TiO_2 (M = Ca, Sr and Ba) have been investigated systematically. The MO−TiO_2 binary oxides (1:1 molar ratio) were synthesized by adopting a co-precipitation method from the corresponding chloride precursors by in situ hydrolysis with urea and calcined at various temperatures from 723 to 1073 K. A nominal 10 wt.% V_2O_5 was deposited over the calcined (773 K) MO−TiO_2 supports by a wet impregnation method. The synthesized catalysts were characterized using X-ray diffraction (XRD), Raman spectroscopy (RS), X-ray photoelectron spectroscopy (XPS), thermogravimetry–differential thermal analysis (TG–DTA) and BET surface area techniques. The MO−TiO_2 composite oxides exhibited reasonably high-specific surface area and high-thermal stability retaining titania-anatase phase up to 1073 K treatment temperature. The impregnated V_2O_5 over MO−TiO_2 binary oxides remained in a highly dispersed form. A preferential interaction between the basic MO and the dispersed V_2O_5 lead to the formation of MVO_3 at higher calcination temperatures. The surface acid–base properties of the prepared samples were examined for the conversion of cyclohexanol to cyclohexanone/cyclohexene under normal atmospheric pressure. All the investigated samples were found to exhibit interesting catalytic properties.

Keywords: TiO_2-anatase; Vanadium oxide; Dispersion; Acid–base properties; Cyclohexanol

1. Introduction

Oxidation catalysts are always the subjects of interest because of their significant role both in the production and destruction of desired and undesired products respectively by oxidation reactions, partial or complete [1–3]. In this context, considerable attention has been focused on the synthesis, characterization and evaluation of various new catalyst systems for increasing newer applications. Among industrial oxidation catalysts, supported vanadium oxides share an important position due to their efficiency in several heterogeneous catalytic processes including *ortho*-xylene partial oxidation, ammoxidation of hetero-aromatic compounds, selective catalytic reduction (SCR) of NO_x, oxidative dehydrogenation of alkanes and so on [1–9]. Among supported vanadium oxide catalysts, the V_2O_5/TiO_2 combination has gained paramount importance.

Titania (TiO_2) has been widely studied because of its extensive use as a support as well as catalyst due to its inherent characteristics such as high-dielectric constant, better oxygen sensitivity and photoelectric properties [10,11]. Orthorhombic brookite, tetragonal anatase and tetragonal rutile are the three natural phases reported for titania crystallization [12]. Some properties of TiO_2 are very sensitive to its structure. Anatase phase is chemically and optically active making it suitable for catalysts and supports. Rutile phase is known to bear highest refractive index and UV-absortivity for which it finds uses in paints, pigments and UV-absorbents [12]. For most commercial SCR and selective oxidation applications, TiO_2 has been employed as the support on which the active chemical species including V_2O_5, WO_3 and MoO_3 were impregnated [13,14]. Since anatase is a metastable titania polymorphs, it tends to transform into rutile phase decreasing its surface area thereby inducing a loss of catalytic activity [13]. The anatase to rutile transformation has been reported to be a major cause of deactivation in titania-based catalysts [15]. The stabilization of TiO_2-anatase phase can be achieved by changing its surface or bulk composition by incorporating various additive atoms [12]. Such combination

* Corresponding author. Tel.: +91 40 2716 0123; fax: +91 40 2716 0921.
E-mail addresses: bmreddy@iict.res.in, mreddyb@yahoo.com (B.M. Reddy).

1381-1169/$ – see front matter © 2007 Elsevier B.V. All rights reserved.
doi:10.1016/j.molcata.2007.07.018

catalysts for example, $V_2O_5/Ga_2O_3-TiO_2$, $V_2O_5/La_2O_3-TiO_2$ and $V_2O_5/CaO-TiO_2$ possessing acid–base and redox characteristics were reported to exhibit better catalytic properties for various reactions [16–18]. Addition of CeO_2 and CuO to TiO_2 matrix has also been reported to improve the thermal stability and specific surface area of the titania thereby inducing better catalytic activity [12].

The present investigation was undertaken against the above background. In this systematic study the influence of same group alkaline earth metal oxides namely CaO, SrO and BaO on the phase stability and catalytic properties of TiO_2 has been examined. A homogeneous co-precipitation method was adopted to make the desired $MO-TiO_2$ binary oxide combinations (M = Ca, Sr and Ba; 1:1 molar ratio) and calcined at various temperatures from 723 to 1073 K. A nominal 10 wt.% V_2O_5 was also deposited over the calcined (723 K) $MO-TiO_2$ supports and subjected to various calcination temperatures. Physicochemical properties of all synthesized catalysts were investigated by means of X-ray diffraction, Raman spectroscopy, X-ray photoelectron spectroscopy, differential thermal analysis and BET surface area techniques. To assess the acid–base properties, conversion of cyclohexanol to cyclohexanone and cyclohexene was performed. The competitive dehydration/dehydrogenation reaction of cyclohexanol is considered as a universal test reaction for evaluation of acid–base properties of various solid catalysts [19–21]. It is a known fact that both surface acid–base characteristics and redox properties of catalysts greatly influence the selective oxidation or oxidative dehydration reactions of commercial significance [22,23].

2. Experimental

2.1. Catalyst preparation

All mixed oxide supports (1:1 molar ratio based on oxides) investigated in the present study were prepared by a homogeneous co-precipitation method using urea as hydrolyzing agent. An appropriate amount of cold $TiCl_4$ (Fluka, AR grade) was initially digested in cold concentrated HCl and subsequently diluted with deionized water. To this aqueous solution the required quantity of $BaCl_2{\cdot}2H_2O$ (Loba Chemie, GR grade) or $SrCl_2{\cdot}6H_2O$ (Loba Chemie, GR grade) or $CaCl_2{\cdot}2H_2O$ (Loba Chemie, GR grade), dissolved separately in deionized water, was added. An excess solid urea (Loba Chemie, AR grade) with a metal to urea molar ratio of 1:2.5 was also added to this mixture solution for better control of pH and heated to 368 K with vigorous stirring. After about 6 h of heating, a white precipitate was gradually formed as the urea decomposition progressed to a certain extent. In order to make sure complete precipitation, the pH of the solution was increased further by adding dilute ammonia externally. The precipitate was heated for 18–24 h and kept aside for 4 days to facilitate aging. The co-precipitate thus obtained was filtered off and washed thoroughly with deionized water until free from anion impurities. The obtained cake was oven dried at 383 K for 12 h and calcined at various temperatures from 723 to 1073 K for 6 h in air atmosphere.

A nominal 10 wt.% V_2O_5 was deposited on various mixed oxide supports by adopting a wet impregnation method. To impregnate V_2O_5, the requisite quantity of ammonium metavanadate (Fluka, AR grade) was dissolved in aqueous oxalic acid solution (2 M). To this clear solution, the finely powdered calcined (723 K) mixed oxide support was added. The excess water was evaporated on a water-bath with constant stirring and the resulting material was oven dried at 383 K for 16 h and subsequently calcined at various temperatures from 723 to 1073 K for 5 h in a closed muffle furnace in flowing oxygen atmosphere. The rate of heating (as well as cooling) was always maintained at 10 K min^{-1}. In the text all the catalysts containing 10 wt.% V_2O_5 were labeled as VCT (V_2O_5/CaO–TiO_2), VST (V_2O_5/SrO–TiO_2) and VBT (V_2O_5/BaO–TiO_2), and the pure supports as CT (CaO–TiO_2), ST (SrO–TiO_2) and BT (BaO–TiO_2), respectively for the sake of convenience during discussion.

2.2. Catalyst characterization

X-ray powder diffraction patterns were recorded on a Siemens D-5000 diffractometer, using monochromated Cu Kα (0.15418 nm) radiation and standard recording conditions. The XRD phases present in the samples were identified with the help of the ASTM powder data files. The Raman spectra were recorded at ambient temperature on a Nicolet FT-Raman 960 spectrometer using the 1064 nm exciting line (∼600 mV) of a Nd:YAG laser (Spectra Physics). The wavenumber values obtained from spectra are accurate to within 2 cm^{-1}. The XPS measurements were made on a VG Scientific Lab 210 spectrometer by using Mg Kα (1253.6 eV) radiation as the excitation source. Charging of catalyst samples was corrected by setting the binding energy of the adventitious carbon (C 1s) at 284.6 eV. The XPS analysis was done at room temperature and pressures typically in the order of less than 10^{-6} Pa.

The TG–DTA analysis was performed on a Mettler Toledo TG–SDTA apparatus. Uncalcined samples were heated from ambient temperature to 1173 K under nitrogen flow. The sample weight was *ca.* 12 mg and the heating rate was 10 K min^{-1}. The specific surface areas of the samples were determined on a Micromeritics Gemini 2360 instrument by N_2 physisorption at liquid nitrogen temperature. Before measurements, the samples were oven dried at 393 K for 12 h and flushed in situ with He gas for 2 h.

2.3. Catalytic activity

To study the acid–base properties of various samples, the vapour phase reaction of cyclohexanol to cycohexanone/cyclohexene was investigated under normal atmospheric pressure, in a down flow fixed bed differential micro-reactor, at different temperatures from 623 to 723 K. For each run ∼2 g of catalyst sample was secured between two plugs of quartz wool inside the glass reactor and above the catalyst bed filled with glass chips in order to act as preheating zone. The reactor was placed vertically inside a tubular furnace, which can be heated electrically. The reactor temperature was monitored by

a thermocouple with its tip located near the catalyst bed and connected to a temperature indicator-cum-controller. Prior to reaction in order to facilitate activation of the catalyst, it was heated in a flow of dry air (30 mL min^{-1}) at 723 K for 5 h. After the activation, the temperature was adjusted to the desired level and cyclohexanol was fed from a motorized syringe pump into the vaporizer where it was allowed to mix uniformly with air before entering the preheating zone of the reactor. The reaction was performed at a cyclohexanol feed rate of 1 mL h^{-1} in dry air flow of 600 cm^3 h^{-1}. There was a slight decrease in the conversion after start of the reaction. After about 1 h, the activity was quite stable and the data were collected under these conditions. The liquid products collected through the spiral condensers in ice cooled freezing traps were analyzed by a gas chromatograph using OV-17 column and FID detector. The main reaction products obtained were cyclohexanone, cyclohexene and phenol along with some traces of unidentified products.

3. Results and discussion

The N_2 BET surface areas of various binary oxide supports and the corresponding vanadia impregnated samples calcined at different temperatures are presented in Table 1. All the prepared mixed oxide supports in the present study exhibited reasonably a high-surface area. Due to sintering phenomenon, the surface areas decreased with increasing calcination temperature. It has been observed that specific surface area of CT is minimum while that of BT is maximum and the ST being intermediate. The same trend is observed in the case of vanadia impregnated samples (VCT < VST < VBT). Very interestingly, the specific surface areas of the investigated mixed oxides increased with increase in the size of the alkaline earth metal. This may be due to the formation of more open structures with increase in the size of the alkaline earth metal cations (ionic radii: Ca^{2+} = 142 pm, Sr^{2+} = 132 pm and Ba^{2+} = 149 pm). Decrease in the surface areas of the supports can be observed after impregnation with vanadium pentoxide. This is due to the penetration of the dispersed vanadium oxide into the pores of the support thereby narrowing its pore diameter and blocking some of the micropores [16]. Additionally, the solid-state reactions between the acidic dispersed vanadium oxide and the basic counterparts of the support (CaO, SrO and BaO) may also contribute to the observed decrease in the BET surface areas [24].

Table 1
BET surface areas (m^2 g^{-1}) of prepared catalysts calcined at different temperatures

Sample	Calcination temperature (K)			
	723	923	1073	1273
CT	77	64	26	21
VCT	42	25	16	9
ST	96	55	30	15
VST	62	20	10	3
BT	101	61	40	19
VBT	68	37	18	8

The thermogravimetric analyses of all samples in the range of ambient to 1173 K at a ramp of 10 K min^{-1}, revealed two major weight-loss peaks. The TGA profiles are found to be slightly different in the peak maxima temperature regions. The first major low-temperature peak in the 323–398 K range was primarily due to the loss of non-dissociative adsorbed water, as well as water held on the surface by hydrogen bonding. The second weight-loss peak in the range 468–678 K is due to the dehydroxylation of the surface. In the case of the CaO–TiO_2 sample, the weight loss from ambient to 773 K was ~18% and from 773 to 1173 K, it was only 2%. This indicates that over the temperature range 773–1173 K, the CaO–TiO_2 binary oxide is quite stable in terms of phases and chemical composition. In the case of SrO–TiO_2, the loss of sample weight from ambient to 773 K was ~21% and from 773 to 1173 K, ~3%. Thus, in the range of 773–1173 K, the SrO–TiO_2 binary oxide seems to be thermally quite stable. A weight loss of ~23% was noted in the case of BaO–TiO_2 sample from ambient to 773 K and thereafter, a small loss of ~3% was observed from 773 to 1173 K reflecting good thermal stability. For all the vanadia impregnated samples two endothermic regions were noted after the water loss peak at around 473 K. These are mainly due to the decomposition of ammonium metavanadate and the carbonates of the alkaline earth metals. Also there is a possibility of solid solution formation as a result of reaction between the dispersed vanadium oxide and the corresponding supports.

The XRD profiles of various binary oxide supports and vanadium oxide impregnated samples calcined at 723 and 1073 K are shown in Figs. 1 and 2, respectively. In case of the supports, broad diffraction lines due to TiO_2-anatase phase (JCPDS File No. 21-1272) as well as peaks arising due to the presence of $CaCO_3$ (JCPDS File No. 24-27), $SrCO_3$ (JCPDS File No. 5-418) and $BaCO_3$ (JCPDS File No. 11-97) are mainly observed. However, in the case of BT sample the XRD patterns pertaining to TiO_2-anatase phase are more intense and the characteristic lines due to $BaCO_3$ are less prominent. XRD results reveal that alkaline earth metal carbonates are readily formed during the preparation process and not completely decomposed into their oxides within the investigated calcination temperatures. It is worth mentioning here that these materials were prepared by urea hydrolysis method. The dissolved urea in water decomposes into ammonia and CO_2 at ~368 K. Thus generated CO_2 reacts with the alkaline earth metals to form the stable carbonates in addition to their amorphous hydroxides. In particular, no XRD lines due to TiO_2-rutile phase are noted, which is an important observation from the point of view of their catalytic applications. The XRD patterns of vanadia-loaded samples are more intense and exhibit similar diffraction patterns similar to that of the corresponding supports. No crystalline vanadia features are evident leading to the conclusion that vanadia is present in a highly dispersed amorphous state on the surface of the supports. From Fig. 2, it is clear that with increase of calcination temperature from 723 to 1073 K, in case of VCT and VST samples, an improvement in the intensity of the lines due to TiO_2-anatase phase can be observed along with the formation of corresponding titanates (JCPDS File Nos. 22-153 and 6-520, respectively). In case of VBT sample, in addition to titanate formation (JCPDS

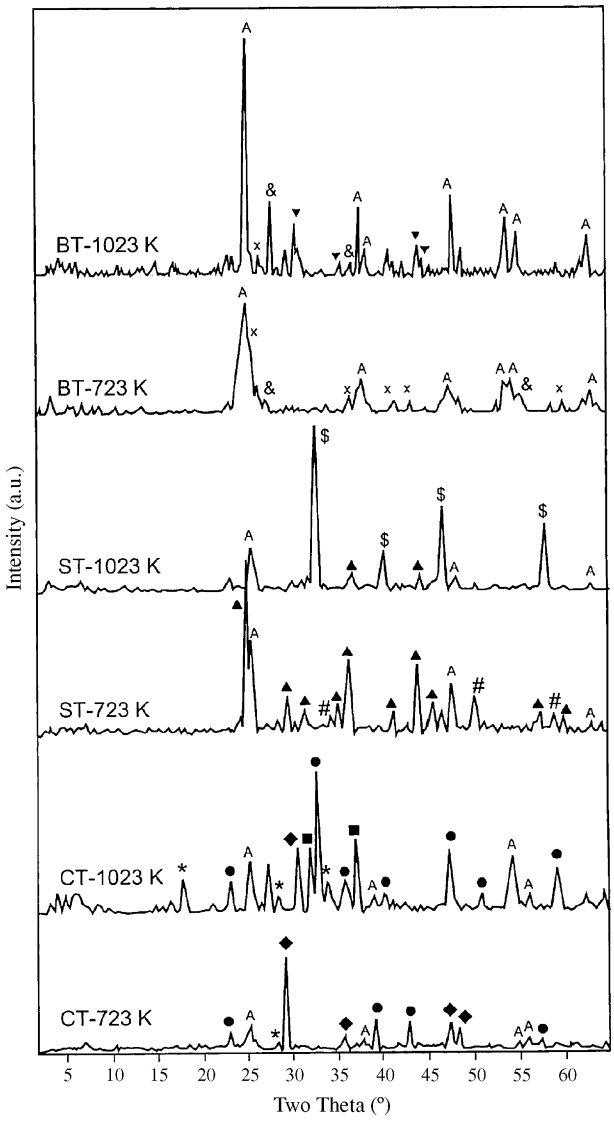

Fig. 1. X-ray powder diffraction profiles of CT, ST and BT samples calcined at 723 and 1073 K, respectively: (A) peaks due to TiO_2-anatase; (♦) peaks due to $CaCO_3$; (■) peaks due to CaO; (●) peaks due to $CaTiO_3$; (*) peaks due to $Ca(OH)_2$; (▲) peaks due to $SrCO_3$; (#) peaks due to SrO; ($) peaks due to $SrTiO_3$; (×) peaks due to $BaCO_3$; (&) peaks due to BaO; (▼) peaks due to $BaTiO_3$.

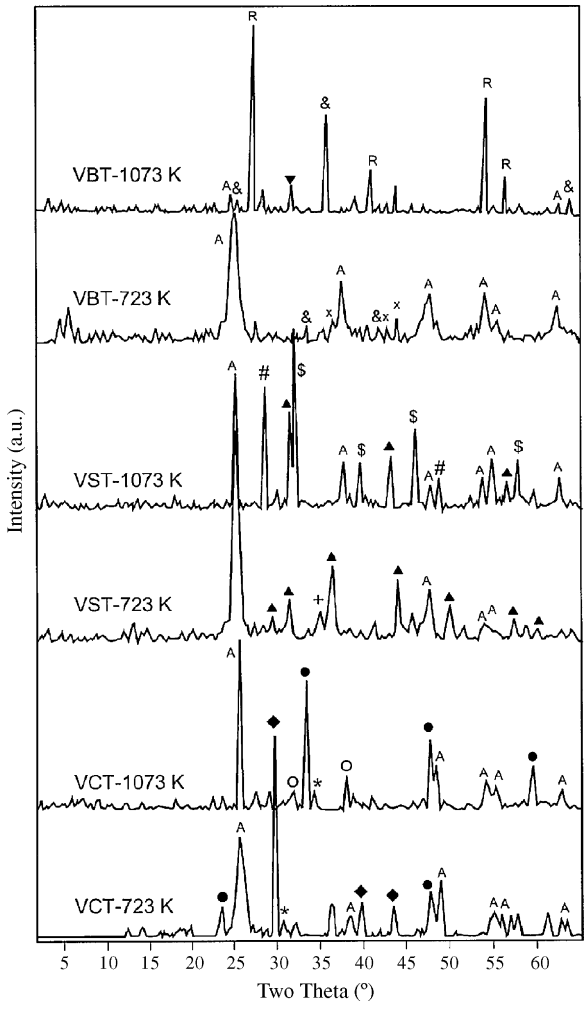

Fig. 2. X-ray powder diffraction profiles of VCT, VST and VBT samples calcined at 723 and 1073 K, respectively: (A) peaks due to TiO_2-anatase; (♦) peaks due to $CaCO_3$; (■) peaks due to CaO; (●) peaks due to $CaTiO_3$; (*) peaks due to $Ca(OH)_2$; (◯) peaks due to $CaVO_3$; (▲) peaks due to $SrCO_3$; (#) peaks due to SrO; ($) peaks due to $SrTiO_3$; (×) peaks due to $BaCO_3$; (&) peaks due to BaO; (▼) peaks due to $BaTiO_3$; (R) peaks due to TiO_2-rutile.

File No. 5-626), TiO_2-anatase to rutile (JCPDS File No. 21-1276) transformation at 1073 K is also noted. Here too, no XRD lines due to crystalline vanadium oxide are observed even up to the calcination temperature of 1073 K. Up to this temperature range, in the case of VCT, the $CaVO_3$ (JCPDS File No. 14-127) formation was also observed. A few lines with very less intensity, due to $Ca(OH)_2$, were also noted (JCPDS File No. 4-733). In all cases, characteristic lines corresponding to basic oxide phases namely CaO (JCPDS File No. 4-777), SrO (JCPDS File No. 6-520) and BaO (JCPDS File No. 7-233) were also observed.

The Raman spectra of various samples calcined at 723 K are shown in Fig. 3. The TiO_2-anatase phase crystallizes in the space group $I4_1/amd$ and the rutile phase in the $P4_2/mnm$ space group respectively [25]. As per the literature, the anatase phase possesses Raman features at 144, 199, 399, 520, and 643 cm^{-1} and the rutile phase at 144, 148 and 611 cm^{-1}, respectively [12,26]. The Raman bands of all the support oxides are identical in position, and show all characteristic features of TiO_2-anatase phase. No characteristic Raman bands due to TiO_2-rutile or MO or M–Ti-oxides could be observed. The CT and ST samples and their vanadia counterparts bear sharp bands at ~1080 and ~284 cm^{-1} which are the characteristic peaks for their corresponding alkaline earth metal carbonates [18]. These peaks are not present in case of barium containing samples due to less presence of $BaCO_3$ in these samples as revealed by XRD analysis. The major peak of crystalline V_2O_5 assigned to the V=O stretching mode appears at 995 cm^{-1} [26]. No Raman bands due to crystalline vanadia phase are identifiable. The intensity of the Raman bands pertaining to TiO_2-anatase increased gradually from CT to BT as the intensity of Raman band depends on the morphology of the samples. The Raman spectra of vanadia-impregnated samples are similar to the spectra of the parent supports. The Raman measurements are thus inline with the observations made from XRD studies.

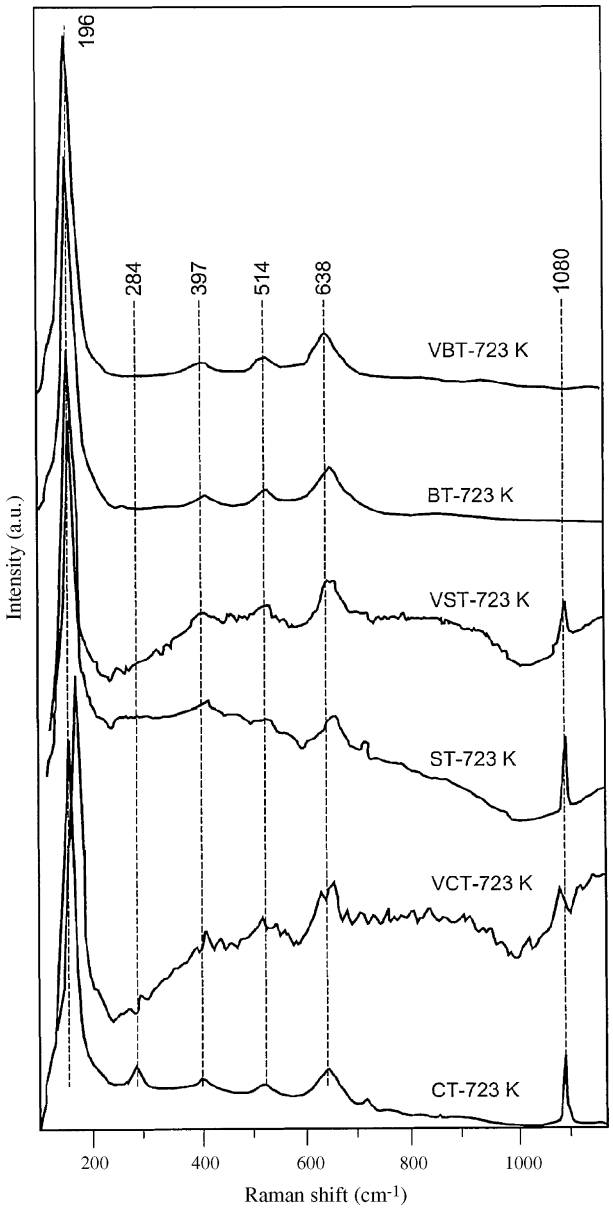

Fig. 3. Raman spectra of various prepared samples calcined at 723 K.

The representative XPS bands of O 1s, Ti 2p, Ca 2p, Sr 3d, Ba 3d and V 2p pertaining to various binary oxide supports and the corresponding vanadia-loaded samples are shown in Figs. 4–7, respectively. These figures clearly indicate that the XPS bands are highly sensitive to the composition of the mixed oxide supports and also to the presence of V_2O_5 on their surfaces. The O 1s peak of all catalyst systems (Fig. 4a and b) is, in general, more complicated due to the overlapping contribution of oxygen from alkaline earth metal oxides and titanium oxide in the case of supports and also vanadium oxide in the case of V_2O_5-containing catalysts. The broad nature of the peaks reveals the non-equivalence of surface oxygen ions. Mainly, two distinct oxygen peaks are observed for both the series of catalyst systems calcined at different temperatures. It can be easily assigned that the intense peak at lower binding energy is due to the oxygen atoms that are bound to Ti (i.e., TiO_2) and the one at higher binding energy mainly belonging to the corresponding alkaline earth metal oxide, judging from the difference in the electronegativity of the elements involved [24]. In the case of pure supports, the binding energy of the most intense O 1s peak is almost constant whereas in case of vanadia impregnated samples a small shift in the binding energy towards higher values is noted. It may be due to a different degree of dispersion of vanadium oxide on the surface of the supports. Also a clear increase in the binding energy for vanadia-impregnated samples is noted with increase in calcination temperature, which can be attributed to the segregation of vanadium oxide on the support surface [27].

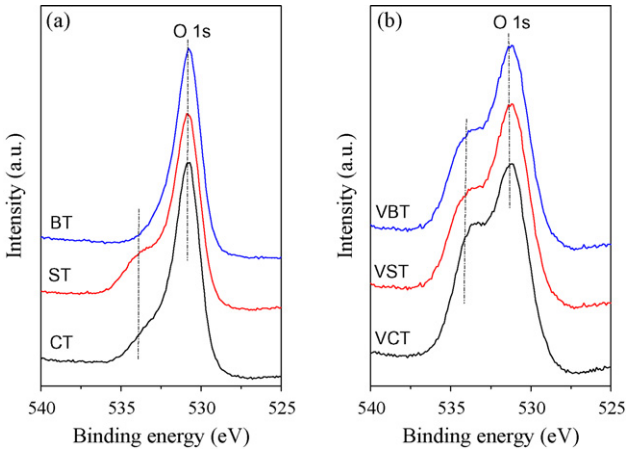

Fig. 4. O 1s XPS spectra of (a) CT, ST and BT and (b) VCT, VST and VBT samples calcined at 723 K.

As shown in Fig. 5a and b, the binding energy of the Ti $2p_{3/2}$ photoelectron peak for all samples ranged between 458.0 and 459.3, 458.5 and 460.4, 459.2 and 460.9 eV, which agree well with the values reported in the literature [28–30]. An extensive broadening of the Ti 2p peak, in line with O 1s peak, is also noted in the case of samples calcined at 723 K. The broadening of the Ti 2p peak is mainly due to redistribution of various components in the catalyst system under the influence of high-temperature calcination. A total redistribution of various components is expected in the case of vanadia-containing

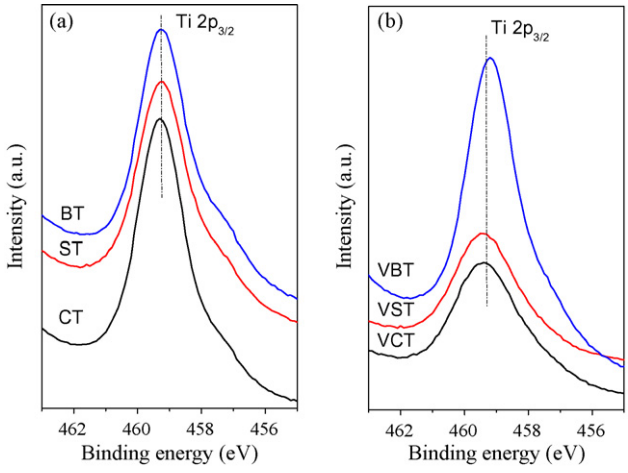

Fig. 5. Ti 2p XPS spectra of (a) CT, ST and BT and (b) VCT, VST and VBT samples calcined at 723 K.

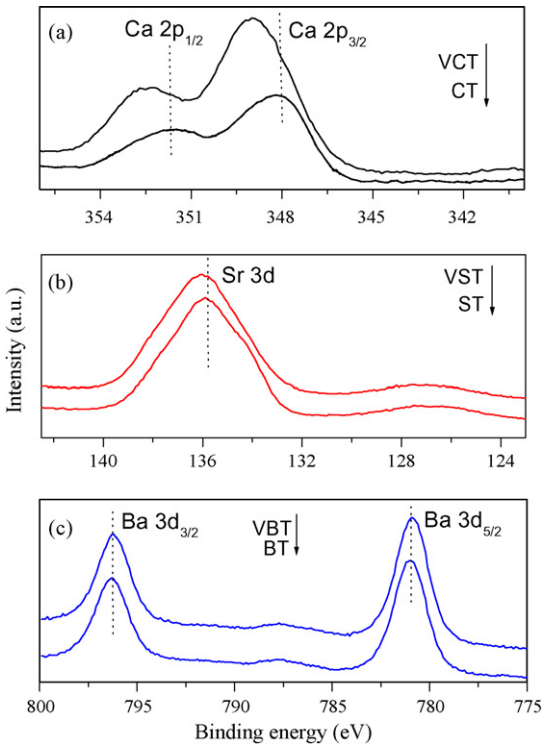

Fig. 6. Ca 2p, Sr 3d and Ba 3d XPS spectra of (a) CT and VCT, (b) ST and VST, and (c) BT and VBT samples calcined at 723 K.

samples due to a strong interaction between the acidic V_2O_5 and the basic alkaline earth metal oxides to form the stable MVO_3 compounds. Interestingly, Ti 2p binding energy values are found to be constant showing the existence of Ti in the same oxidation state (+4) in all the samples. The increase in intensity of the Ti 2p peak with increase in calcination temperature is due to a better crystallization of samples.

Fig. 6a–c shows the binding energies of the Ca 2p photoelectron peaks at ~347.96 and ~351.66 eV for Ca $2p_{3/2}$ and Ca $2p_{1/2}$, respectively showing binding energy difference of ~3.5 eV. Very broad photoelectron peaks at ~135.0 eV in case of Sr 3d could be observed (here, contributions from $3d_{5/2}$ and $3d_{1/2}$ are not resolved). The Ba 3d photoelectron peaks are observed at ~780.96 and ~796.28 eV for Ba $3d_{5/2}$ and Ba $3d_{3/2}$ lines, respectively giving binding energy difference of ~15.3 eV, which agree well with the spectra reported in the literature [28,29]. The intensity of the peaks observed is almost independent of the calcination temperature in the case of supports. It indicates that the chemical state of metal is same in the supports. However, in the case of VCT, VST and VBT samples increase in the Ca 2p, Sr 3d and Ba 3d binding energies and intensity of the peaks with increasing calcination temperature is noted. The increase in the electron binding energy and the peak intensity changes are primarily due to the formation of MVO_3 compounds and sintering.

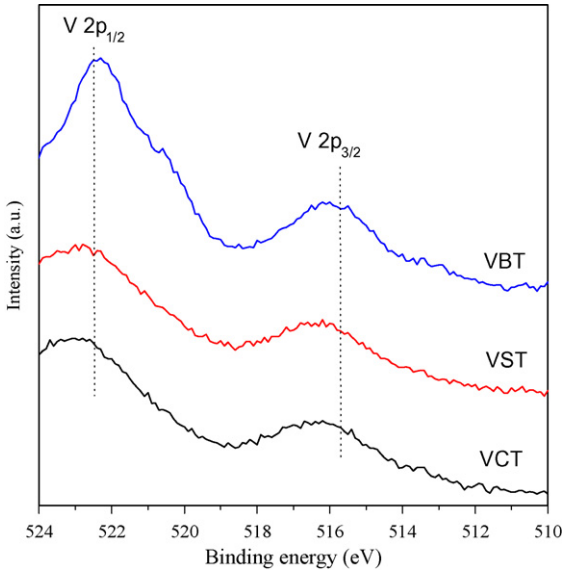

Fig. 7. V 2p XPS spectra of VCT, VST and VBT samples calcined at 723 K.

Fig. 7 shows the V 2p photoelectron peaks of the above catalyst samples calcined at 723 K. The V 2p photoelectron peaks are observed at ~515.7 and ~522.5 eV for V $2p_{3/2}$ and V $2p_{1/2}$, respectively (showing binding energy difference of ~6.8 eV), which is in agreement with literature reports [28,29,31]. A significant broadening and decrease in the intensity of the V 2p line can be noted. The broadening of the XPS peaks can be attributed to various factors as envisaged earlier which include (i) the presence of more than one type of V^{5+} or V^{4+} species with different chemical characteristics, which cannot be discerned by ESCA, and (ii) the electron transfer between the active component and the support (metal–support interaction) [32]. With increase in calcination temperature, a gradual increase in the intensity and a shift in binding energy values were observed. This may be due to a strong interaction between the dispersed vanadium oxide and the basic component of the MO–TiO_2 leading to the formation of MVO_3 [27]. As presented in the figure the sample calcined at 723 K appears to contain a mixture of MVO_3 compound (V^{4+} species) and a highly dispersed V-oxide phase (V^{5+} state) on the surface of the support. The formation of MVO_3 compounds may also lead to the broadening of the V 2p peak. Literature reveals that V_2O_5 on TiO_2 accelerates the anatase to rutile phase transformation and during this process some dispersed V_2O_5 gets reduced and incorporate into the rutile structure forming $V_xTi_{1-x}O_2$ rutile solid solution [2]. It appears from the present investigation that interaction of basic oxides with V_2O_5 inhibits the formation of $V_xTi_{1-x}O_2$ by forming MVO_3 compounds thereby facilitating the titania-anatase phase stabilization. The XPS results thus synchronize with the observations noted from XRD and Raman measurements.

The activity results for cyclohexanol conversion over various samples calcined at 723 K and investigated between 623 and 723 K under normal atmospheric pressure are presented in Fig. 8. Good to excellent conversions were obtained over all the samples, BT being the best one. Conversion of cyclohexanol increased with increasing reaction temperature. Interestingly, all catalysts followed the same trend and there is no big difference in the activity among various supports. The large difference in the activity between the impregnated and unimpregnated samples is due to acid–base characteristics of the catalysts and the difference within the impregnated samples may be due to

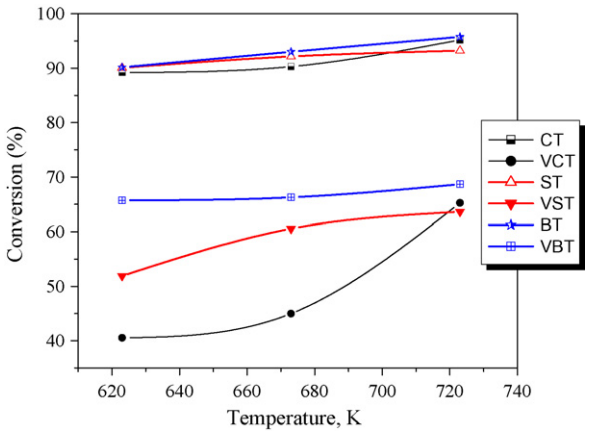

Fig. 8. Conversion of cyclohexanol over various prepared samples at different temperatures and normal atmospheric pressure.

the difference in the degree of compound formation between the dispersed vanadia and the alkaline earth metal oxides. The corresponding selectivity results are shown in Fig. 9. As can be noted from the figure, the product selectivity distribution depends on the nature of the sample investigated. Two types of reactions namely dehydration and dehydrogenation are happening simultaneously and the dehydration results cyclohexene and dehydrogenation leads to cyclohexanone. As can be noted from Fig. 9, more selectivity towards cyclohexanone is observed over the supports and cyclohexene over the vanadia-impregnated samples. The product selectivity is highly dependent on the surface acid–base properties of the catalysts. It is an established fact that cyclohexene selectivity is related to the surface acidity and the cyclohexanone selectivity to surface basicity of the catalysts [33]. As per the selectivity results, the supports exhibit more basic character whereas vanadia impregnated samples possess more acidic properties. Apparently, BT shows highest cyclohexanol to cyclohexanone conversion. The formation of more amounts of cyclohexanone over the support oxides than on the vanadia impregnated samples also could be due to the presence of more surface oxygen anions, which are expected to be generated in the preparation stage [17]. The preparation procedure adopted in the present investigation, where an oxide or hydrous oxide sample is formed by condensation and polymerization of the hydroxylated metal ions precipitated from an aqueous solution, there is a possibility of formation of coordinatively unsaturated metal cations and oxygen anions on the surface of the resulting composite oxides [18]. Literature reveals that exposed coordinatively unsaturated metal cations and oxygen anions on the surface act as Lewis acid and Brønsted base sites [1,2]. The dehydration product, cyclohexene formation can be correlated with Brønsted acid sites and the dehydrogenation product, cyclohexanone, could be correlated directly with the basic sites [34]. After vanadia impregnation on the surface of the support oxides, a significant improvement in the selectivity towards cyclohexene is noted. It is reported that V_2O_5 is a typical acid possessing only Brønsted acid sites and produces cyclohexene as the sole product in the reaction of cyclohexanol [34]. The increase in selectivity towards cyclohexene on vanadia-impregnated catalysts also gives an impression that vanadium oxide is covering the surface of the supports resulting in the formation of dispersed vanadium oxide species. With the impregnation of vanadium oxide, the exposed coordinatively unsaturated sites are drastically decreased on the surface and hence significant lowering of the cyclohexanone selectivity is observed [18]. A close observation of Fig. 9 reveals that higher selectivity to cyclohexanone and cyclohexene over supports and vanadia impregnated samples, respectively is observed at lower

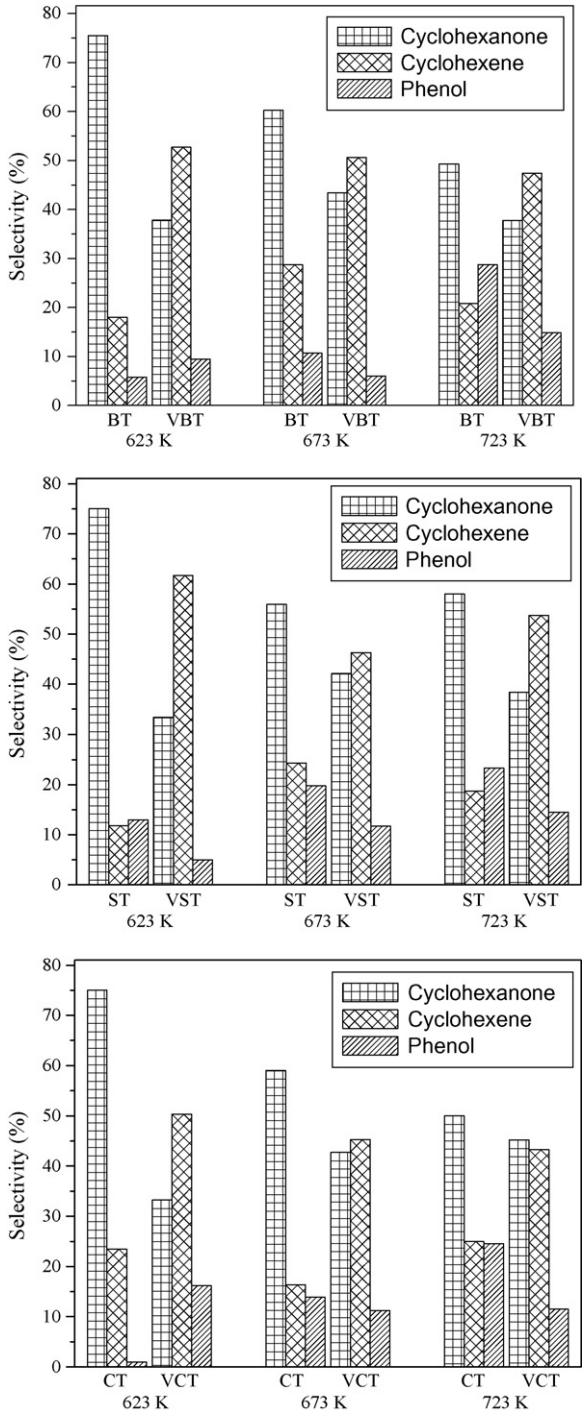

Fig. 9. Selectivity results of cyclohexanol conversion to different products over various prepared samples at different temperatures and normal atmospheric pressure.

reaction temperatures. The activity results reveal clearly that vanadia impregnated samples contain more acidic sites on the surface than that of pure supports. The time-on-stream experiments were carried out using 723 K calcined samples at the reaction temperature of 723 K to understand the stability of the catalysts. The products collected after regular intervals of time up to 16 h, manifested almost same activity results in terms of conversion and selectivity. A negligible decrease (∼2%) in conversion could be noted after 16 h of reaction time and the change in product selectivity distribution was even less than that. The activity was also tested for 10% V_2O_5/TiO_2 under same experimental conditions. The conversion was found to be in the range of 45–56% as we change the reaction temperature from 623 to 723 K and the product selectivity was dominated by cyclohexene. In this case also with increase in reaction temperature conversion was found to increase. The comparatively low conversion may be due to the involvement of some parts of dispersed vanadia and TiO_2 to form the most feasible amorphous $V_xTi_{(1-x)}O_2$ (rutile solid solution) as established in the literature [2,24].

The dispersion of the vanadium oxide as well as its structure can be understood on the basis of different acid–base character of various supports [35,36]. It has been observed that the tendency of VO_x species to be dispersed on the surface of metal oxide supports is related to its basicity. In other words, the agglomeration of VO_x species to form V_2O_5 crystallites is favoured with the acidic character of the support. Due to the acidic character of the vanadium oxide, which possesses a point of zero surface charge (pzc) at pH 1.4, it can easily react with basic oxides, whereas a weaker interaction with another acidic oxide will favour agglomeration of the VO_x units to form V_2O_5. From XRD, Raman and XPS observations, no crystalline V_2O_5 was observed for all the supports. The strong basic properties of CaO, SrO and BaO in the binary oxide supports are primarily responsible for this observation. As basic strength increases in the order CaO < SrO < BaO, the agglomeration of V_2O_5 is inhibited in the same trend and as a result more dispersed V_2O_5 is present as one moves from CaO to BaO.

4. Conclusions

This study confirms that basic oxides namely CaO, SrO and BaO when incorporated to TiO_2, play an effective role in titania-anatase phase stabilization. As basic strength increases in the order CaO < SrO < BaO, the agglomeration of V_2O_5 is inhibited in the same trend. The impregnated V_2O_5 remains in a highly dispersed and amorphous state over all the supports. At elevated temperatures, thermally quite stable corresponding titanates and vanadates of the basic oxides are formed. The formation of alkaline earth metal vanadates inhibits the formation of the most feasible $V_xTi_{(1-x)}O_2$ (rutile solid solution) at higher calcination temperatures. All the samples show good to excellent cyclohexanol conversion. The alkaline earth metal containing titania supports exhibit more cyclohexanone selectivity and the corresponding V_2O_5 loaded catalysts exhibit more cyclohexene selectivity reflecting their basic and acidic properties, respectively.

Acknowledgements

P.S. and G.T. thank CSIR, New Delhi for the award of Junior Research Fellowship. Financial support received from Department of Science and Technology, New Delhi under SERC Scheme (SR/S1/Pc-31/2004).

References

[1] D.J. Hucknall, Selective Oxidation of Hydrocarbons, Academic Press, London, 1974.
[2] G.C. Bond, S.F. Tahir, Appl. Catal. 71 (1991) 1.
[3] M.A. Banares, Catal. Today 51 (1999) 319, and references therein.
[4] I.E. Wachs, R.Y. Saleh, S.S. Chan, C.C. Chersich, Appl. Catal. 15 (1985) 339.
[5] P. Cavalli, F. Cavani, I. Manenti, F. Trifiro, Catal. Today 1 (1987) 245.
[6] B.N. Reddy, B.M. Reddy, M. Subrahmanyam, J. Chem. Soc., Faraday Trans. 87 (1991) 1649.
[7] H. Bosch, F. Janssen, Catal. Today 2 (1988) 369.
[8] K. Chen, A. Khodakov, J. Yang, A.T. Bell, E. Iglesia, J. Catal. 186 (1999) 325.
[9] X. Wang, I.E. Wachs, Catal. Today 96 (2004) 211.
[10] J.E.G.J. Wijnhiven, W.L. Vos, Science 281 (1998) 802.
[11] K.I. Hadjiivanov, D.G. Klissurski, Chem. Soc. Rev. 25 (1996) 61.
[12] M.S.P. Francisco, V.R. Mastelaro, Chem. Mater. 14 (2002) 2514.
[13] J.M.G. Amores, V.S. Escribano, G. Busca, V. Lorezelli, J. Mater. Chem. 4 (1994) 965.
[14] S.T. Choo, S.D. Yim, I.S. Nam, S.W. Ham, J.B. Lee, Appl. Catal. B: Environ. 44 (2003) 237.
[15] R.Y. Saleh, I.E. Wachs, S.S. Chan, C.C. Chersich, J. Catal. 98 (1986) 102.
[16] B.M. Reddy, I. Ganesh, B. Chowdhary, Chem. Lett. (1997) 1145.
[17] B.M. Reddy, I. Ganesh, J. Mol. Catal. A: Chem. 169 (2001) 207.
[18] B.M. Reddy, K.J. Ratnam, P. Saikia, J. Mol. Catal. A: Chem. 252 (2006) 238.
[19] S. Jaenicke, Catal. Surveys Asia 9 (3) (2005) 173, and references therein.
[20] F.M. Bautista, J.M. Campelo, A. Garcia, D. Luna, J.M. Marinas, R.A. Quiros, A.A. Romero, Appl. Catal. A: Gen. 243 (2003) 93.
[21] T. Radhica, S. Sugunan, Catal. Commun. 7 (2006) 528.
[22] J. Kijenski, A. Baiker, Catal. Today 5 (1989) 1.
[23] M. Ai, J. Mol. Catal. A: Chem. 114 (1996) 3.
[24] B.M. Reddy, I. Ganesh, E.P. Reddy, J. Phys. Chem. B 101 (1997) 1769.
[25] M. Kosmulski, Adv. Colloid Interf. Sci. 99 (2002) 255.
[26] B.M. Reddy, P. Lakshmanan, A. Khan, C.L. Cartes, T.C. Rojas, A. Fernandez, J. Phys. Chem. B 109 (2005) 1781.
[27] B.M. Reddy, K.N. Rao, G.K. Reddy, P. Bharali, J. Mol. Catal. A: Chem. 253 (2006) 44.
[28] D. Briggs, M.P. Seah (Eds.), Practical Surface Analysis, Auger and X-ray Photoelectron Spectroscopy, vol. 1, 2nd ed., Wiley, New York, 1990.
[29] C.D. Wagner, W.M. Riggs, L.E. Davis, J.F. Moulder, in: G.E. Muilenberg (Ed.), Handbook of X-ray Photoelectron Spectroscopy, Perkin-Elmer Corporation, Minnesota, 1978.
[30] Q. Wang, R.J. Madrix, Surf. Sci. 474 (2001) L213.
[31] V.I. Bukhtiyarov, Catal. Today 56 (2000) 403.
[32] B.M. Reddy, B. Chowdhary, I. Ganesh, E.P. Reddy, T.C. Rojas, A. Fernandez, J. Phys. Chem. B 102 (1998) 10176.
[33] D. Martin, D. Duprez, J. Mol. Catal. 118 (1997) 113.
[34] C.P. Bezouhanova, M.A. Al-Zihari, Catal. Lett. 11 (1991) 245.
[35] U. Schart, M. Schrami-Marth, A. Wokaun, A. Balker, J. Chem. Soc., Faraday Trans. 87 (1991) 3299.
[36] G. Deo, I.E. Wachs, J. Phys. Chem. 95 (1991) 5889.